Nonlinear State-Observer Techniques for Sensorless Control of Automotive PMSM's, including Load-Torque Estimation and Saliency

B.S. Bhangu, C.M. Bingham

Electrical Machines and Drives Group, Dept of Electronic & Electrical Engineering,
University of Sheffield, Mappin Street, Sheffield S1 3JD, UK
Tel. +44 (0) 114 2225195; Fax. +44 (0) 114 2225196
Corresponding author: email elp99bsb@sheffield.ac.uk

Keywords

Automotive applications, Brushless drives, DSP, Estimation techniques, Permanent magnet motors, Sensorless control, Vector control

Abstract

The paper investigates various non-linear observer-based rotor position estimation schemes for sensorless control of permanent magnet synchronous motors (PMSMs). Attributes of particular importance to the application of brushless motors in the automotive sector, are considered e.g. implementation cost, accuracy of predictions during load transients, the impact of motor saliency and algorithm complexity. Emphasis is given to techniques based on model linearisation during each sampling period (EKF); feedback-linearisation followed by Luenberger observer design based on the resulting 'linear' motor characteristics; and direct design of non-linear observers.

Although the benefits of sensorless commutation of PMSMs have been well expounded in the literature, an integrated approach to their design for application to salient machines subject to load torque transients remains outstanding.

Furthermore, this paper shows that the inherent characteristics of some non-linear observer structures are particularly attractive since they provide a phase-locked-loop (PLL)-type of configuration that can encourage stable rotor position estimation, thereby enhancing the overall sensorless scheme. Moreover, experimental results show how operation through, and from, zero speed, is readily obtainable. Experimental results are also employed to demonstrate the attributes of each methodology, and provide dynamic and computational performance comparisons.

Introduction

The automotive sector is currently accelerating through a transitional phase of replacing hydraulic and belt-driven auxiliary components of the drive train with direct-drive electric motors; the perceived power source for such units being batteries/peak-power buffers, fuel cells, and, more immediately, IC-engine/electric hybrid combinations. Consequently, the power-to-weight advantages and thermal characteristics attributed to permanent magnet (PM) brushless motors are making them the preferred option for the electro-mechanical and electro-hydraulic actuation and servo systems. However, intense economic constraints, product volumes and manufacture/motor parameter tolerance issues consistent with the automotive industry, has meant that the cost and component count attributed to the requirement for rotor position sensors for the increasing number of machines envisaged for auxiliaries, is leading to increased interest in sensorless position estimation schemes. Furthermore, where applications call for custom motor designs, the omission of a rotor position sensor provides the additional benefit of allowing an increase in the active length of the rotor/stator, thereby increasing the power/torque obtained for a given volume envelope. Nevertheless, before a sensorless solution can be considered successful, the automotive sector requires that the following key issues are also addressed:

- Minimal algorithm complexity/code length
- Accurate rotor position estimates during dynamic load disturbances—no transient loss of information.
- Robustness to parameter tolerances.

The first issue directly relates to the economics of utilising extra capacity on existing minimal-cost computational hardware (there is little point in replacing position sensors with relatively expensive processing hardware), whilst the remaining issues concern, respectively, operational performance of the motor and the consequences of volume manufacture.

For servo-type applications, and applications where electromagnetic torque ripple and audible noise have a significant impact on overall product quality, vector control schemes, Fig.1, are preferred. In this case, sensorless operation is achieved by utilising only motor terminal quantities to accurately estimate rotor position.

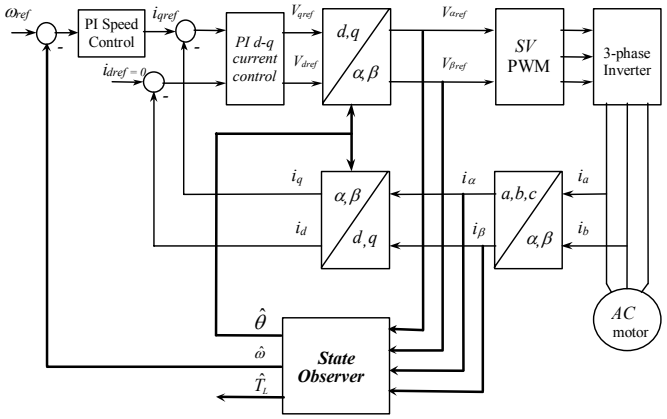

Fig. 1. Classical *d-q* torque/speed motor control with observed rotor position

The situation is further complicated for cost-critical applications by the preferred use of PMSMs that possess significant saliency, and the requirement to accommodate substantial transient load torque variations. The realisation of appropriate 'sinusoidal' sensorless schemes therefore presents a significant challenge for the designer in this field, and, whilst various observer-based techniques have been proposed in literature [1,2,3,4], an integrated approach to their design for application to salient machines subject to load torque transients, remains outstanding. Here then, various distinct non-linear position estimation methodologies, are investigated, to address these key drivers.

Nonlinear Observer-based Schemes

To provide a comparison of the performance attributes of each presented methodology, including the addition of load torque estimation and the impact of including saliency dynamics, the well documented Extended Kalman Filter (EKF) [1], which relies on linearising the motor model about the current operating point during at each sampling period, is considered as a benchmark. The EKF is employed for observation of nonlinear systems in the hope that some of the optimal properties attributed to the Kalman Filter for linear systems, might transfer to the non-linear counterpart over small deviations from each nominal operating point. Although the effectiveness of the EKF has been previously demonstrated under experimental conditions by a number of authors [5,6,7], major drawbacks for critical automotive drive systems are the lack of formal tuning and stability procedures, and the computational overhead necessary for implementation, due to the requirement for calculating the Jacobians at each sample step.

Next, an observer scheme that takes account of the full non-linear dynamic characteristics of the motor, is considered; the underlying principles being first introduced in [2]. Since these methods do

not require calculation of the Jacobians at each sample step, the computation overhead is significantly reduced. Both aforementioned techniques are provisionally developed in the α-β stator-fixed reference frame, Eq.(1) where the inputs are $u=[v_\alpha, v_\beta]^T$ and the measured outputs are $y=[i_\alpha, i_\beta]^T$ and R_s, L_s, K_e and K_t are respectively, the phase resistance, synchronous inductance, back-emf and torque constants; J is the rotor inertia, B is the motor viscous friction, ω is the rotor angular velocity, θ is the rotor position and p denotes the number of pole pairs. Finally, a third methodology is developed solely in the *d-q* reference frame Eq.(2), where the inputs are $u=[v_d, v_q]^T$, and the measured outputs are $y=[i_d, i_q]^T$, which employs an inner-loop non-linear feedback (linearisation) controller to render the system as essentially linear for the subsequent design of an observer using classical Luenberger techniques [3]. The unobservability of the rotor position in the *d-q* frame, is addressed, and a correction scheme is employed to account for offset, drift and divergence due to unknown initial conditions, measurement noise and modelling errors. Experimental results provide a relative comparison of the dynamic attributes of each methodology. Fig. 2 highlights the structural differences between each observer scheme, however, for brevity, the reader is referred to the cited texts for full mathematical derivations.

$$\frac{d}{dt}i_\alpha = -\frac{R_s}{L_s}i_\alpha + \frac{K_e}{L_s}\omega\sin\theta + \frac{v_\alpha}{L_s}$$
$$\frac{d}{dt}i_\beta = -\frac{R_s}{L_s}i_\beta - \frac{K_e}{L_s}\omega\cos\theta + \frac{v_\beta}{L_s}$$
$$\frac{d}{dt}\omega = \frac{K_t p}{J}(i_\beta\cos\theta - i_\alpha\sin\theta) - \frac{B}{J}\omega$$
$$\frac{d}{dt}\theta = \omega$$

(1)

$$\frac{d}{dt}i_d = -\frac{R_s}{L_s}i_d + \omega i_q + \frac{v_d}{L_s}$$
$$\frac{d}{dt}i_q = -\frac{R_s}{L_s}i_q - \omega i_d - \frac{K_e}{L_s}\omega + \frac{v_q}{L_s}$$
$$\frac{d}{dt}\omega = \frac{K_t p}{J}i_q - \frac{B}{J}\omega$$
$$\frac{d}{dt}\theta = \omega$$

(2)

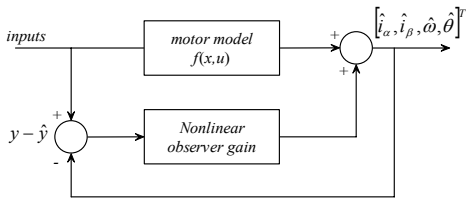

(a) Nonlinear observer

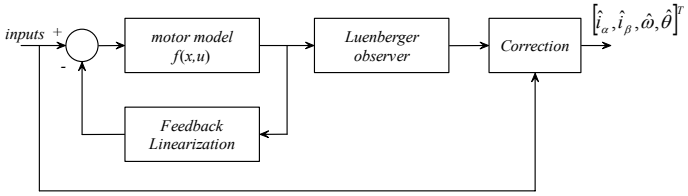

(b) Luenberger observer

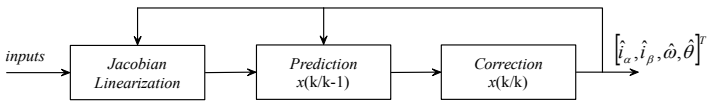

(c) EKF

Fig. 2 Structure of observer schemes

Operation from Zero Speed

An attribute of the EKF and Luenberger observers, is their ability to maintain observer stability at zero speed, following initial convergence of the state estimates. By way of example, the experimental results depicted in Figs. 3 & 4 show both methodologies controlling an automotive 1.5kW, 6-pole, PMSM servomotor, with a base speed of 2500rpm, operating to zero speed, and subsequently accelerating from zero speed after a delay of ≈8 seconds. Although position error substantially

increases around zero speed, it does not destabilise the observer or prevent the motor from subsequently starting.

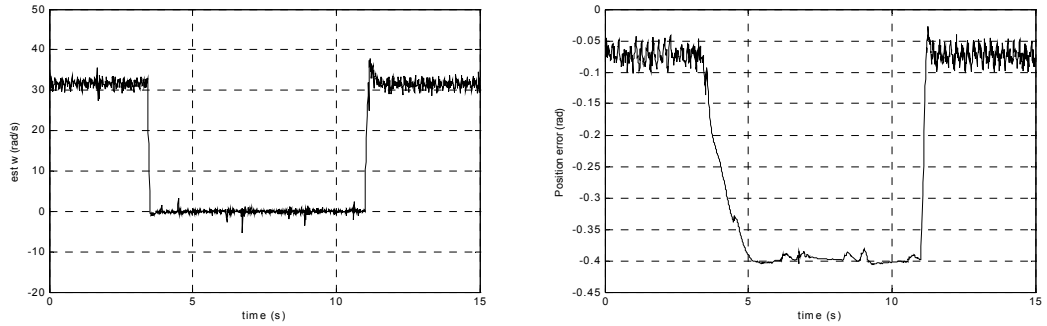

(a) (b)

Fig. 3. Experimental data from Luenberger Observer a) estimated speed b) position error

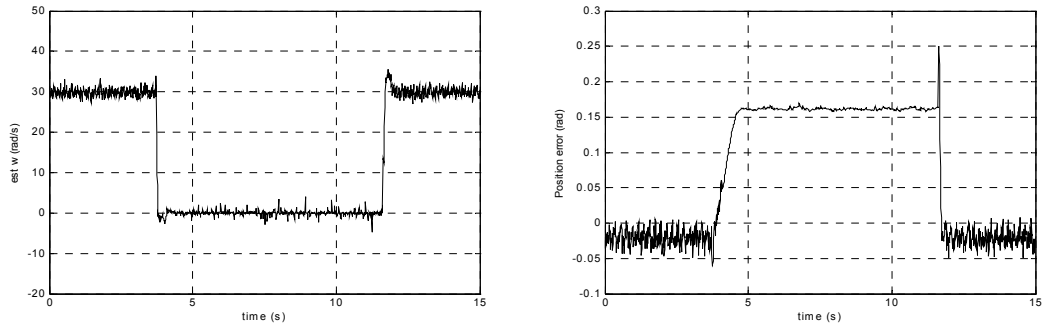

(a) (b)

Fig. 4. Experimental data from EKF a) estimated speed b) position error

Impact of Employing Estimates of Load Torque

A comparative study of the proposed observer schemes under no load conditions, has been previously reported in [8]. Here, an additional state, pertaining to estimates of load torque, is included by augmenting the state equations with $dT_L/dt=0$, where T_L represents the estimated load torque disturbance, with a view to both enhancing the accuracy of the rotor position estimate, and to enable the possibility of implementing a feedforward speed control scheme for disturbance rejection. The augmented model equations for observer derivation therefore become:

$$\frac{d}{dt}\omega = \frac{K_t p}{J}(i_\beta \cos\theta - i_\alpha \sin\theta) - \frac{B}{J}\omega - \frac{T_L p}{J} \qquad \frac{d}{dt}\omega = \frac{K_t p}{J} i_q - \frac{B}{J}\omega - \frac{T_L p}{J}$$

$$\frac{d}{dt}T_L = 0 \qquad \frac{d}{dt}T_L = 0$$

Applying a step load of 1Nm to the motor at ≈ *0.2*s, without including the load torque dynamics results in significant steady-state error, as shown by the experimental results in Fig. 5, for each observer scheme. Conversely, Fig. 6 shows the significant improvement in rotor position accuracy that can be obtained when the load estimates are included. However, whilst it is seen that all methodologies are able to induce similar closed-loop dynamics, there can be significant differences in the computational complexity of each technique. Table 1 provides an indication of computational complexity, normalised to the requirements of the EKF.

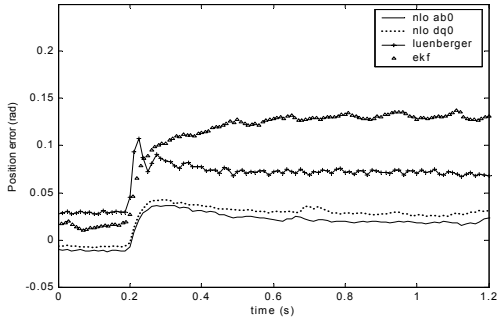

Fig. 5. Position error (experimental) after a 1Nm load disturbance applied at 0.2s without load torque included in observer

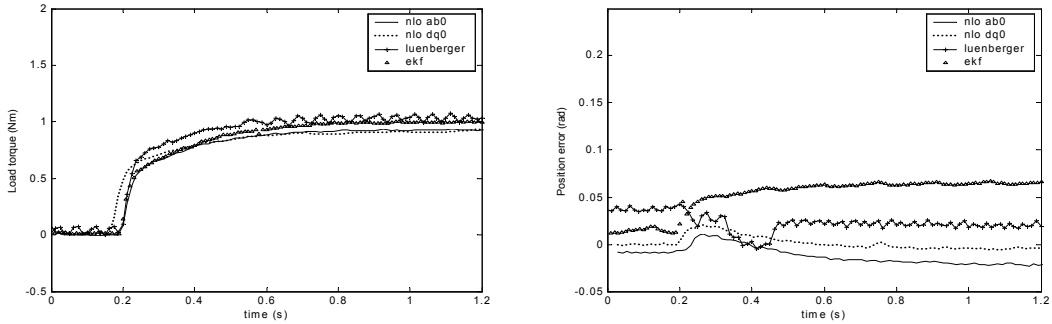

(a) (b)

Fig. 6. Experimental results (a) Observed load torque (b) Position error when load torque is observed

	No Load Observation		Incorporating Load Observation	
	Computation time	Memory requirement	Computation time	Memory requirement
EKF	1	1	1.04	1.13
Nonlinear observer in $\alpha\beta0$ frame	0.07	0.36	0.09	0.44
Nonlinear observer dq0 frame	0.06	0.38	0.08	0.47
Luenberger observer	0.05	0.31	0.06	0.34

Table. I Comparison of computational complexity normalised to EKF

Impact of Saliency on Rotor Position Estimates

The use of flat, buried magnets may be preferred in the design of some custom motors for cost-critical applications, since they can be cheaper to manufacture and can produce similar flux densities to surface mounted magnets whilst requiring less bulk material. A consequence however, is that the direct and quadrature inductances, L_d and L_q, respectively, are no longer equal, differing often by up to 30%. Employing nonlinear observers on buried magnet machines without incorporating the effects of saliency can be significantly detrimental to the accuracy of rotor position estimates, as the simulation results of Fig. 7(a) show, where, even under no-load conditions, observer estimates can diverge unstably. However, whilst increasing observer complexity, incorporating saliency into the observer model allows stability to be maintained, Fig. 7(b). It can be further shown that convergence and accuracy are also enhanced by the inclusion of load torque estimation.

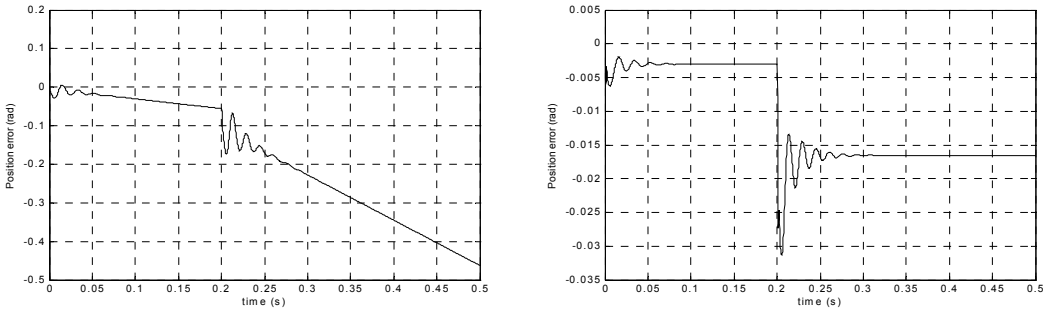

(a) (b)

Fig. 7. Simulation results from salient machine model (a) Position error without saliency accounted for in observer (b) Position error with salient dynamics included in observer.

Implementing Saliency into an EKF-based Observer Scheme

The mathematical model of an Interior Permanent Magnet Synchronous Machine (IPMSM) in the *dq*0 reference frame is given by (3), and, in the stator-fixed $\alpha\beta 0$ reference frame, by (4):

$$\begin{bmatrix} v_d \\ v_q \end{bmatrix} = \begin{bmatrix} R_s + pL_d & -\omega L_q \\ \omega L_d & R_s + pL_q \end{bmatrix} \begin{bmatrix} i_d \\ i_q \end{bmatrix} + \begin{bmatrix} 0 \\ K_e \omega \end{bmatrix} \tag{3}$$

$$\begin{aligned} \begin{bmatrix} v_\alpha \\ v_\beta \end{bmatrix} &= R_s \begin{bmatrix} i_\alpha \\ i_\beta \end{bmatrix} + \begin{bmatrix} L_0 + L_1 \cos 2\theta & L_1 \sin 2\theta \\ L_1 \sin 2\theta & L_0 - L_1 \cos 2\theta \end{bmatrix} \bullet \frac{d}{dt} \begin{bmatrix} i_\alpha \\ i_\beta \end{bmatrix} \\ &\quad + \omega \begin{bmatrix} -2L_1 \sin 2\theta & 2L_1 \cos 2\theta \\ 2L_1 \cos 2\theta & 2L_1 \sin 2\theta \end{bmatrix} \begin{bmatrix} i_\alpha \\ i_\beta \end{bmatrix} + K_e \omega \begin{bmatrix} -\sin\theta \\ \cos\theta \end{bmatrix} \end{aligned} \tag{4}$$

where

$$L_0 = \frac{L_d + L_q}{2}, \quad L_1 = \frac{L_d - L_q}{2} \tag{5}$$

Eq.(4) can be further simplified by the definition of equivalent inductances:

$$L_\alpha = L_0 + L_1 \cos 2\theta, \quad L_\beta = L_0 - L_1 \cos 2\theta, \quad L_{\alpha\beta} = L_1 \sin 2\theta \tag{6}$$

and considering the third term to have negligible impact, providing:

$$\begin{bmatrix} v_\alpha \\ v_\beta \end{bmatrix} = R_s \begin{bmatrix} i_\alpha \\ i_\beta \end{bmatrix} + \begin{bmatrix} L_\alpha & L_{\alpha\beta} \\ L_{\alpha\beta} & L_\beta \end{bmatrix} \bullet \frac{d}{dt} \begin{bmatrix} i_\alpha \\ i_\beta \end{bmatrix} + K_e \omega \begin{bmatrix} -\sin\theta \\ \cos\theta \end{bmatrix} \tag{7}$$

Although much simplified, the motor model in the stator fixed reference frame Eq.(7) now consists of inductances that vary as a sinusoidal function of 2θ, which significantly complicate the calculation of Jacobians for the EKF, and increases computational overhead. To reduce such problems, a motor model is required with inductances that are not a function of rotor position. The *dq*0 reference frame therefore provides a convenient platform. Re-arranging (3) provides:

$$\begin{bmatrix} v_d \\ v_q \end{bmatrix} = \begin{bmatrix} R_s + pL_d & -\omega L_q \\ \omega L_q & R_s + pL_d \end{bmatrix} \begin{bmatrix} i_d \\ i_q \end{bmatrix} + \begin{bmatrix} 0 \\ \left(L_d - L_q\right)\left(\omega i_d - \frac{d}{dt} i_q\right) + K_e \omega \end{bmatrix} \tag{8}$$

In the $\alpha\beta 0$ frame we equivalently have:

$$\begin{bmatrix} v_\alpha \\ v_\beta \end{bmatrix} = \begin{bmatrix} R_s + pL_d & \omega\left(L_d - L_q\right) \\ -\omega\left(L_d - L_q\right) & R_s + pL_d \end{bmatrix} \begin{bmatrix} i_\alpha \\ i_\beta \end{bmatrix} + \left(\left(L_d - L_q\right)\left(\omega i_d - \frac{d}{dt} i_q\right) + K_e\omega \right) \begin{bmatrix} -\sin\theta \\ \cos\theta \end{bmatrix} \tag{9}$$

whose elements now consist of constant inductances. A minor drawback associated with such an implementation is that $dq0$ currents are required in the $\alpha\beta 0$ frame coordinates. However, this is achieved at no extra computational cost since the vector control employed requires generation of currents in $dq0$ frame. Note, however, that the second term in (9) requires the rate of change of q-axis current. The complete IPMSM dynamic model in the stationary $\alpha\beta 0$ reference frame is represented as:

$$\begin{aligned} f(x) &= \frac{d}{dt} \begin{bmatrix} i_\alpha \\ i_\beta \\ \omega \\ \theta \end{bmatrix} \\ &= \begin{bmatrix} -\frac{R_s}{L_d} i_\alpha - \frac{\omega}{L_d} i_\beta \left(L_d - L_q\right) + \left[\left(L_d - L_q\right)\left(\omega i_d - \frac{d}{dt} i_q\right) + K_e\omega \right] \frac{\sin\theta}{L_d} + \frac{v_\alpha}{L_d} \\ -\frac{R_s}{L_d} i_\beta + \frac{\omega}{L_d} i_\alpha \left(L_d - L_q\right) - \left[\left(L_d - L_q\right)\left(\omega i_d - \frac{d}{dt} i_q\right) + K_e\omega \right] \frac{\cos\theta}{L_d} + \frac{v_\beta}{L_d} \\ \frac{K_t p}{J} i_q + \frac{3p}{2J}\left(L_d - L_q\right) i_d i_q - \frac{B}{J}\omega - \frac{pT_L}{J} \\ \omega \end{bmatrix} \end{aligned} \tag{10}$$

Assuming the sampling rate is sufficiently fast, we can make the simplifying assumption that $di_q/dt = 0$ over a single sampling interval, for the determination of the Jacobian (11):

$$F\left(x(t)\right) = \left.\frac{\partial f}{\partial x}\right|_{x=x(t)}$$

$$= \begin{bmatrix} -\frac{R_s}{L_d} + \omega L_0 \frac{\sin 2\theta}{2} & -\omega L_0 \cos^2\theta & \frac{K_e}{L_d}\sin\theta + L_0 i_\alpha \frac{\sin 2\theta}{2} - L_0 i_\beta \cos^2\theta & F(1,4) \\ \omega L_0 \sin^2\theta & -\frac{R_s}{L_d} - \omega L_0 \frac{\cos 2\theta}{2} & -\frac{K_e}{L_d}\cos\theta - L_0 i_\beta \frac{\cos 2\theta}{2} + L_0 i_\alpha \sin^2\theta & F(2,4) \\ F(3,1) & F(3,2) & -\frac{B}{J} & F(3,4) \\ 0 & 0 & 1 & 0 \end{bmatrix}$$

$$F(1,4) = \frac{K_e}{L_d}\omega\cos\theta + \omega L_0 i_\alpha \cos 2\theta + \omega L_0 i_\beta \sin 2\theta \tag{11}$$

$$F(2,4) = \frac{K_e}{L_d}\omega\sin\theta + \omega L_0 i_\beta \sin 2\theta + \omega L_0 i_\alpha \sin 2\theta$$

$$F(3,1) = -\frac{K_t p}{J}\sin\theta + \frac{3p}{2J}\left(L_d - L_q\right)\left(-i_\alpha \sin 2\theta + i_\beta \cos 2\theta\right)$$

$$F(3,2) = \frac{K_t p}{J}\cos\theta + \frac{3p}{2J}\left(L_d - L_q\right)\left(i_\alpha \cos 2\theta + i_\beta \sin 2\theta\right)$$

$$F(3,4) = -\frac{K_t p}{J}\left(i_\alpha \cos\theta + i_\beta \sin\theta\right) + \frac{3p}{2J}\left(L_d - L_q\right)\left(-i_\alpha{}^2 \cos 2\theta - 2 i_\alpha i_\beta \sin 2\theta + i_\beta{}^2 \cos 2\theta\right)$$

Implementing Saliency in the Non-Linear Observer Scheme

As with the EKF, the complete IPMSM is modelled in the stationary $\alpha\beta 0$ reference frame whilst incorporating $dq0$ frame inductances (10). To date, the design of the observer is complicated by the lack of formal stability and tuning procedures for selecting the observer gain matrix. However, extending the work given in [2,3], the following change of co-ordinates is proposed to obtain the structure of the non-linear correction term.

$$z = \begin{bmatrix} z_{1s} \\ z_{2s} \end{bmatrix} = T_s(\omega,\theta) = \begin{bmatrix} z_{1a} + z_{1b} \\ z_{2a} + z_{2b} \end{bmatrix} \tag{12}$$

where

$$\begin{aligned} z_{1a} &= -\frac{\omega}{L_d} i_\beta \left(L_d - L_q\right) & z_{1b} &= \frac{1}{L_d}\left[\left(L_d - L_q\right)\left(\omega i_d - \frac{d}{dt} i_q\right) + K_e\omega\right]\sin\theta \\ z_{2a} &= \frac{\omega}{L_d} i_\alpha \left(L_d - L_q\right) & z_{2b} &= -\frac{1}{L_d}\left[\left(L_d - L_q\right)\left(\omega i_d - \frac{d}{dt} i_q\right) + K_e\omega\right]\cos\theta \end{aligned} \tag{13}$$

giving

$$\begin{aligned} z_{1s} &= \frac{K_e\omega}{L_d}\sin\theta + \omega i_d \frac{L_d - L_q}{L_d}\sin\theta - \frac{d}{dt} i_q \frac{L_d - L_q}{L_d}\sin\theta - \omega i_\beta \frac{L_d - L_q}{L_d} \\ z_{2s} &= -\frac{K_e\omega}{L_d}\cos\theta - \omega i_d \frac{L_d - L_q}{L_d}\cos\theta + \frac{d}{dt} i_q \frac{L_d - L_q}{L_d}\cos\theta + \omega i_\beta \frac{L_d - L_q}{L_d} \end{aligned} \tag{14}$$

The first term on RHS of both z_{1s} and z_{2s} corresponds to the component of nonlinear term associated with the construction of the nominal non-salient observer. The remaining terms correspond to the influence of saliency. Substituting (12) into (10) we obtain the output, $\dot{y}$ as a linear function of the new state $z = \left[z_{1s}, z_{2s}\right]^T$ and the inputs $\left[v_\alpha, v_\beta\right]^T$.

$$\begin{aligned} \frac{d}{dt} i_\alpha &= -\frac{R_s}{L_d} i_\alpha + z_{1s} + \frac{v_\alpha}{L_d} \\ \frac{d}{dt} i_\beta &= -\frac{R_s}{L_d} i_\beta + z_{2s} + \frac{v_\beta}{L_d} \end{aligned} \tag{15}$$

The time derivative of (12), is determined, and the motor model now obtained in the new coordinates enables the non-linear correction term (gain matrix) to be obtained in a similar manner to the non-salient case.

Interestingly, for many automotive applications, the overall effect of saliency i.e. $L_d - L_q \neq 0$ may be negligible, and have only a very minor influence on the observer dynamics when compared to the dominant effects of other motor parameters. Furthermore, it is known that the q-axis inductance varies inversely to q-axis current, hence, at high load, the q-axis inductance will converge towards the d-axis inductance, so that the effect of saliency is reduced at high load. By way of example, the experimental results depicted in Figs. 8 and 9 show, respectively, the dynamic response of the non-salient, and full salient observer schemes on an automotive servomotor with 30% saliency. It is clear that, in this case, the added complexity of employing the full salient dynamics in the observer does not significantly enhance position estimation accuracy.

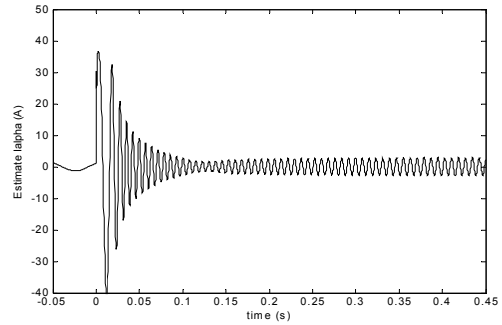

(a)

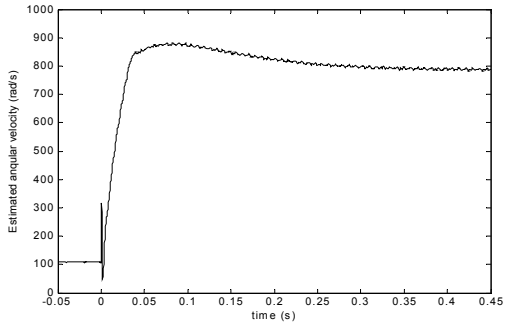

(b)

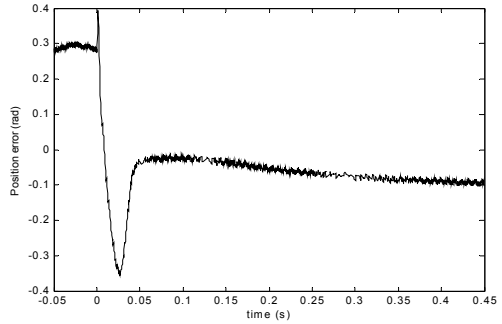

(c)

Fig. 8. Experimental results: Non salient observer
(a) estimated I_α, (b) estimated speed
(c) position error

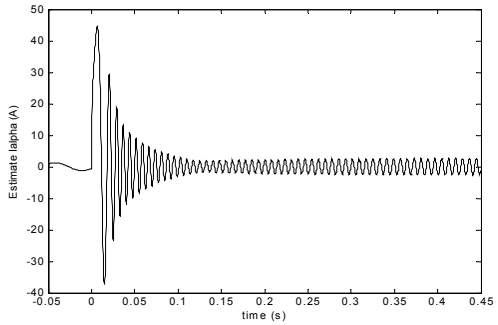

(a)

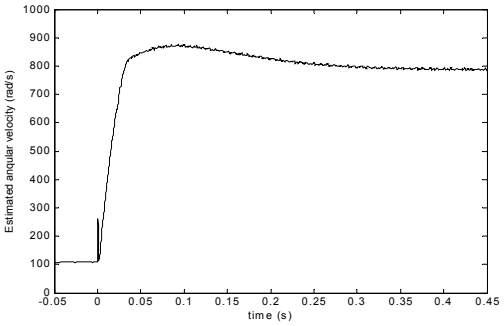

(b)

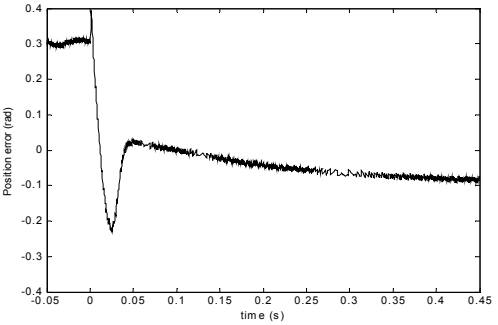

(c)

Fig. 9. Experimental results: Salient observer
(a) estimated I_α, (b) estimated speed
(c) position error

Fig. 10 demonstrates experimentally the effect on position error when the salient motor is subject to a step load disturbance of 1Nm, without incorporating an explicit estimate of load torque. It is evident from the results that the structure of observers implemented on the salient machine results in increased robustness of the estimates.

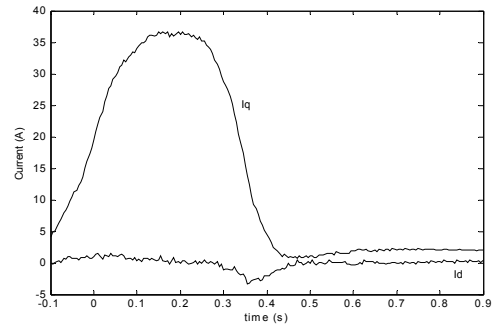

(a)

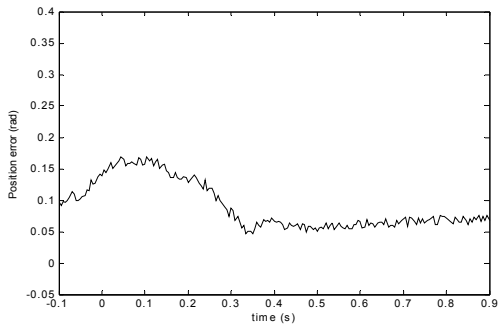

(b)

Fig. 10. Salient observer experimental results a) Measured *dq0* currents b) Position error

Stability Features of Observer/Motor Combination

A feature of model-based sensorless observer schemes employed for closed-loop vector control is that the combined dynamics of the observer and motor can inherently provide a corrective speed/position estimation mechanism. The basis for this is that the torque output of a PMSM motor varies as a function of the cosine of the position error. By setting the observer feedback gains to zero, a combined dynamic model of motor/observer combination is depicted in Fig. 11(a), based on the effect that observed position errors have on electromagnetic torque production in the motor, and the dual impact of errors in estimated and actual electromagnetic torque production, on the residuals of the observer.

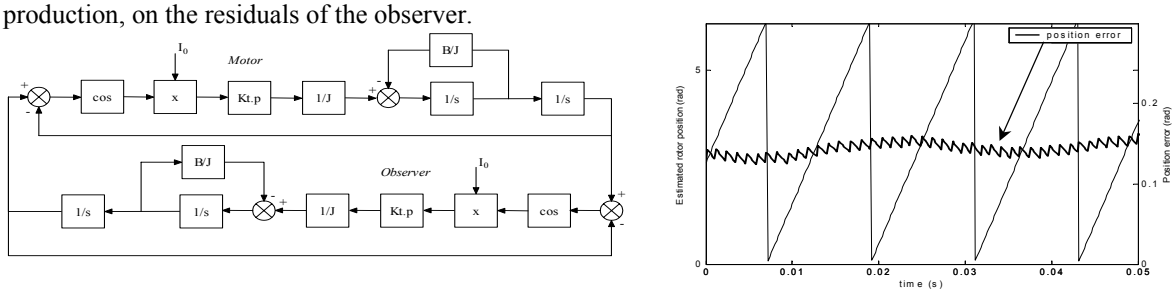

(a) (b)

Fig. 11 (a) Combined observer/motor dynamics with observer gain matrix = 0
(b) estimated & actual (experimental) rotor position, and position error (experimental)

The experimental results of Fig.11(b) show a comparison of measured rotor position, and observer position error, after a transient position error has been forced onto the observer estimates. It can be seen that, whilst a steady-state position error ensues (≈0.15rad), ultimately, the estimated and measured angular speeds converge. This inherent stability characteristic when employing model-based observers is currently being explored to facilitate the generation of more structured techniques for selecting respectively, the covariance matrix employed in the EKF, and the gain matrix for the nonlinear observer.

Conclusions

The paper has described three non-linear observer-based rotor position estimation schemes for sensorless control of PMSMs. Their relative attributes have been discussed to address the specific issues associated with their application to the automotive sector. The execution speed and memory requirements for each technique have been investigated, and the underlying principles of each extended to accommodate load torque estimation and motor saliency. The paper concludes by indicating that model-based observer schemes possess a characteristic that allows convergence of angular velocity estimates when the observer feedback gain is reduced to zero, by virtue of a phase-locked-loop type of motor/observer dynamic structure.

Acknowledgements

The authors would like to thank J. Coles, J. Reeve, A. Szabo and C. Williams of TRW for their assistance, and TRW Conekt and EPSRC (UK) for supporting research student (B. Bhangu) during his PhD studies.

References

[1] A. Bado, S. Bologani, M. Zigliotto "Effective estimation of Speed and Rotor Position of an PM Synchronous Motor Drive by a Kalman Filtering Technique" IEEE Proc. PESC, 1992, pp.951-957.
[2] G. Zhu, A. Kaddouri, L. Dessiant, O. Akhrif "A Nonlinear State Observer for the Sensorless Control of a Permanent-Magnet AC Machine" IEEE Trans. Ind. Electronics, vol. 48, 2001, pp.1098-1108.
[3] D. Hamada, K. Uchida, L. F, Yusivar, S. Wakeo and T. Onuki "Sensorless Control of PMSM using a Linear Reduced Order Observer including Disturbance Torque Estimation" EPE'99 - Lausanne, Waseda University.
[4] J. Solsona and C. Muravchik "A Nonlinear Reduced Order Observer for Permanent Magnet Synchronous Motors" IEEE Trans. Ind. Electronics, vol. 43, 1996, pp.492-497.
[5] R. Dhaouadi, N. Mohan and L. Norum, "Design and Implementation of an Extended Kalman Filter for the State Estimation of a Permanent Magnet Synchronous Motor" IEEE Trans. on Power Electronics, vol. 6, 1999, pp.491-497.
[6] L. Salvatore and S. Stasi, "Application of EKF to parameter and state estimation of PMSM Drive" IEEE Proc., vol. 139, 1992, pp. 155-164.
[7] S. Bolognani, R. Oboe and M. Zigliotto, "Sensorless Full-Digital PMSM Drive With EKF Estimation of Speed and Rotor Position" IEEE Trans. Ind. Electronics, vol. 46, 1999, pp.184-191.
[8] B.Bhangu, C. Williams, C.M. Bingham and J. Coles "EKFs and other Nonlinear State-Estimation Techniques for Sensorless Control of Automotive PMSMs"; Proc. SPEEDAM 2002, pp.C5 33-38, Italy.